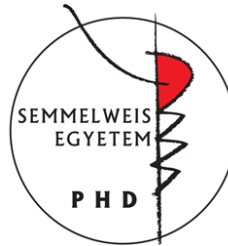


Thyroid hormone action in the central nervous system and peripheral tissues

Ph.D. Thesis

Petra Tímea Mohácsik

Semmelweis University
János Szentágothai Ph.D. School of Neuroscience
Institute of Experimental Medicine,
Hungarian Academy of Sciences



Tutor: Balázs Gereben D.V.M., Ph.D., D.Sc.

Opponents: István Ábrahám M.D., Ph.D., D.Sc.
Orsolya Dohán M.D., Ph.D.

Chairman of committee: Alán Alpár M.D., Ph.D., D.Sc.

Members of committee: Veronika Jancsik Ph.D.
Zita Puskár Ph.D.

Budapest
2016

I. INTRODUCTION

Thyroid hormones (TH) are crucial regulators of many fundamental biological processes e.g. metabolism, neuronal development, growth, stress, reproduction. The daily TH production is tightly controlled by the hypothalamus-pituitary-thyroid (HPT) axis keeping serum T3 levels in the physiological range. Hypophysiotropic thyrotropin releasing hormone (TRH) neurons, the central regulators of the HPT axis, are confined to the medial parvocellular and periventricular subdivision of hypothalamic paraventricular nucleus (PVN) in the rat. TRH axon terminals expand to external zone median eminence (ME), where they secrete the TRH peptide in fenestrated portal capillaries that reaches the thyrotropes in anterior pituitary and evokes thyroid stimulating hormone (TSH) release into peripheral blood to allow TSH-induced stimulation of follicular cells of the thyroid gland. The human thyroid gland produces mainly thyroxin (T4) and only in a lesser extent triiodothyronine (T3). To exert its biological effect the T4 prohormone needs to be activated to T3 that can bind the thyroid hormone receptor (TR). TH regulate their own production via negative feedback at the different levels of the HPT axis. Serum TH levels are relatively stable but TH action occurs predominantly at the tissue level, thus tissue/cell-type specific regulation of TH action needs to be customized by a complex regulatory system. This system involves the transport of TH by various TH transporters, the activation and inactivation by deiodinase enzyme family that allows to customize TH availability, and the regulation of TH action by TH receptors and co-regulators. This tissue-specific system is functionally interlinked with the HPT axis in the hypothalamus. T4 is the TH form that preferentially transported into the brain thus local activation to T3 is especially important, to exert TH action at specific brain regions. In the brain type 2 deiodinase (D2)-mediated TH activation and type 3 deiodinase (D3)-catalyzed inactivation is compartmentalized between glial cells and neurons, respectively. In the hypothalamus, the main T3 generating, D2 expressing cells are tanyocytes, the specialized glial cells, lining the floor and wall of the third ventricle. While the cell bodies of TRH neurons are located in some distance to tanyocytes, the axon terminals and tanyocyte processes are in close proximity in the ME representing a locus where tanyocyte derived T3 can act on TRH neurons. This region represents also an important role in the regulation of other hypophysiotropic neurosecretory neurons like gonadotropin- (GnRH), corticotropin-(CRH), growth hormone- (GHRH) releasing hormone neurons, and somatostatin neurons (SST), which expand their axon terminals to this region and which are well-known target of TH-s.

The reference level of serum TH-s in blood are set by set point formation during development and as a consequence the axis is programmed to keep circulation T3 levels in the desired range. While tight regulation of TH levels during set point formation is crucial and has permanent impact on the entire lifespan, the mechanisms underlying hypothalamic set point formation are largely unknown. Rodents provide a poor model for studies aimed to model the development the human HPT axis due to their strikingly different kinetics of HPT axis development that in rodents is represented by a relatively low developmental stage in the time of prenatal-postnatal transition. In contrast chickens have a relatively well-developed HPT axis at hatching and chicken embryos can separately and directly manipulated in the egg. Similarly to rodents, a time gap between the onset of HPT function and TH-mediated negative feedback also exists during the ontogeny of the chicken embryo. TH activating D2 and the inactivating D3 enzymes regulate hypothalamic TH availability and represent potential regulators of the feedback formation on TRH neurons but ontogenic aspects of this process are poorly understood.

Tissue and cell-type specific regulation of TH action is especially intensely investigated in pathogenesis of non-thyroidal illness syndrome (NTIS) and mechanism of non-shivering thermogenesis (NST) in brown adipose tissue (BAT). Humoral and neuronal inputs to TRH neurons can overwrite normal feedback regulation in specific conditions and challenges like fasting, cold exposure, infection. The NTIS is a striking example of altered regulation of the HPT axis and occurs typically in critically ill patients. It is characterized by falling serum TSH and TH levels that is not followed by the upregulation of the HPT axis. Dissection of altered regulation of TH action in NTIS would be required to better understand the nature and potential treatment of this syndrome. The investigation of possible underlying mechanism of NTIS is frequently studied by bacterial lipopolysaccharide (LPS) induced systemic inflammation model in rodents.

The BAT plays an instrumental role in energy dissipation via NST both in rodents and in human newborns and adults that put this tissue into the frontline of obesity research. The activation of this tissue is regulated by the hypothalamus via the sympathetic nervous system and results in uncoupling protein-1 (UCP1)-mediated mitochondrial uncoupling and heat generation in response to cold. TH and norepinephrine (NE) signalling play a synergistic role in NST and are responsible for sufficient lipogenesis, and adequate thermogenesis during cold exposure. Cold induced increase in D2-mediated local T3 generation facilitates the release of triglycerides from cell stores, accelerates cAMP response and UCP-1 expression. Deeper understanding of the regulation of local TH action in cold stressed BAT would be beneficial to find therapeutic targets for obesity treatment.

II. AIMS

Our studies were performed to better understand the regulation of tissue-specific TH action. Specifically, we aimed to

1. study how onset of negative feedback regulation of the HPT axis occurs
 - determine the period of the onset of TH-mediated negative feedback in the developing chicken hypothalamus
 - identify underlying mechanisms governing set point formation of the HPT axis

2. study the regulation of TH availability in hypothalamic neuroendocrine axes
 - address TH inactivation in parvocellular neurosecretory neurons of rats
 - investigate how regulation of TH availability in neurosecretory neurons responds to challenges in a model of non-thyroidal illness syndrome

3. generate a novel transgenic mouse model allowing the detection of tissue-specific TH action in live animals and tissue samples
 - characterize the Thyroid hormone action indicator mouse model
 - study the hypothalamic pathogenesis of the non-thyroid illness syndrome and interscapular BAT (iBAT) regulation using this model

III. MATERIALS AND METHODS

1.1 *Experimental Animals*

For ontogenic study of HPT axis development white Leghorn chicken embryos and posthatch chickens were obtained from Ceva-Phylaxia (Budapest, Hungary) and Wyverkens (Halle, Belgium).

Posthatch chickens, adult, male Wistar rats (b.w. 220–250 g) and newly generated Thyroid Hormone Action Indicator (THAI) mice (FVB/Ant background) were kept under standard laboratory conditions with food and water *ad libitum*.

1.2 *Recombinant DNA technology and studies in cell cultures*

The recombinant DNA constructs, e.g. the thyroid hormone action indicator construct (THAIC), chicken deiodinase promoter constructs and vectors containing inserts to generate RNA probes for *in situ* hybridization were prepared with standard techniques. DNA fragments were amplified with Taq or Vent polymerase driven polymerase chain reaction (PCR) and cloned to plasmid vectors. The newly prepared recombinant DNA was transformed to bacteria, and the correct clone was amplified in bacterial culture in the presence of antibiotics.

To determine chicken *Dio2* promoter responsiveness to Nkx2.1 U87 human glioma cells were maintained in DMEM supplemented with 10% FBS and were transfected using the calcium-phosphate precipitation method. Briefly, transfection was carried out in a 24-well plate (Corning) using 1600 ng/well total DNA. 20.000 cells were seeded in each well one day before transfection, and the cells were harvested 48 hours later.

To generate THAIC-HEK293T cell line HEK293T cells were cultured in DMEM+10% FBS and transfected with the THAIC targeting construct along with the pcGlobinSB100 transposase encoding vector in the presence of Lipofectamine 2000 reagent (Invitrogen) to allow Sleeping Beauty recombinase assisted genomic integration. Clone selection was performed in the presence of 150 µg/ml zeocin. Clones were cultured for 24 h in charcoal stripped FBS followed by the induction with 100 nM T3 for 24h in the presence of transiently coexpressed mouse TR α .

1.3 *Generation and characterization of Thyroid hormone action indicator (THAI) mouse model*

To generate targeting construct we cloned three copies of a DR-4 TRE (of the human *DIO1* 5' FR) 5' to the *Herpes simplex* virus thymidine kinase (TK) minimal promoter. This DNA

segment was linked upstream of the firefly luciferase coding region containing a codon-optimized and methylation-resistant dCpG Luciferase-ShBle fusion protein upstream of an EF1 pAn polyadenylation cassette. The targeting cassette was flanked by H19 insulators of pWHERE vector (Invivogen) and was cloned to pT2/BH vector (Addgene) between transposase inverted terminal repeat sequences. To generate transgenic mice the pronucleus of fertilized FVB/Ant oocytes was injected with a mixture containing the plasmid harbouring the targeting transposon cassette, along with *in vitro* transcribed mRNA encoding the Sleeping Beauty transposase.

To assess copy number of transgene in the three generated founders (line #4, #18, and #23) fluorescence *in situ* hybridization was performed on lymphocytes, isolated from spleen under aseptic conditions. Insertion site was mapped with Splinkerette PCR technique on genomic DNA. Briefly a specially designed, universal Splinkerette oligonucleotide was used to amplify the region between the 5' end of the transgenic cassette and the first BstYI restriction site, and the fragment was sequenced.

Phenotypic characterization of the founders included measurement of serum TH levels, and body weight, while line #4, 11-week old animals were submitted to indirect calorimetric measurements in metabolic cages (PhenoMaster/LabMaster, TSE Systems GmbH, Bad Homburg, Germany) to determine metabolic parameters, highly dependent on TH status, and body composition analyses using an EchoMRI Whole Body Composition Analyzer (EchoMRI LLC, Houston, TX).

1.4 Modulation and measurement of systemic TH levels

For HPT axis developmental studies we injected E19 and P2 chickens intravenously (chorioallantoic blood vessel or leg vein respectively) with either 1 µg T4, 200 ng T3 or vehicle (saline with 5mM NaOH) as control 8h before sampling.

D3 activity was measured from microdissected ME samples of adult male Wistar rats, injected *i.p.* with 50 µg/of T3/100 g body weight (N=9) or vehicle (N=9) every second days in 8 days.

TH responsiveness of different THAI-Mice tissues was determined *in vitro* from tissue lysates and *in vivo* in live animals using T4 (injected *i.p.* with 5µg/day/mouse of L-T4 or vehicle control for 3 days), T3 (1 µg/g bw of L-T3 for one day) or hypothyroid treatment (0.1% sodium perchlorate and 0.5% methimazole in drinking water for 3 weeks combined with low iodine diet).

Serum free T4 and free T3 levels were measured with AccuLite CLIA Microwells kit according to the manufacturer's instructions. Measurement is based on competitive chemiluminescence enzyme immunoassay methodology in a microplate format.

1.5 *LPS administration, a model of non-thyroidal illness syndrome in rodents*

For double-labelling immunohistochemistry (for D3 and hypophysiotropic peptides) 200g male Wistar rats were treated *i.p.* with LPS (250 µg/ 100g bw; E. coli 0127:B8, Sigma) for 12 hours, and transcardially perfused (see section III/1.6).

THAI-Mice were treated *i.p.* with LPS (150 µg/animal; E. coli 0127:B8, Sigma) and decapitated 6, 8 and 10h after injection. Brain areas (arcuate nucleus + ME and PVN) were microdissected with punch needle from frozen sections placed on pre-cooled glass slides. Tissues were analysed in Taqman real-time quantitative PCR for luciferase and D2 or TRH expression (arcuate nucleus+ME or PVN, respectively).

1.6 *Immunohistochemistry and in situ hybridization*

Control and LPS treated Wistar rat brains were transcardially perfused either with 4% acrolein/2% PFA for detection of TRH or with 4% PFA (for GnRH, GHRH, CRH, TRH and somatostatin). Sections were double-labelled for D3 and hypophysiotropic peptides. After standard histological pretreatments, sections were reacted with the proper primary antibodies, overnight in blocking reagent. Biotinylated D3 antibody was detected with Alexa 488-streptavidine secondary antibody, while primary antibodies against hypophysiotropic peptides were reacted with the appropriate fluorescent (Cy3) conjugated secondary antibodies. Confocal images were taken from the external zone of the ME using 60 X oil immersion objective, scanned by a Radiance 2100 confocal microscope (Bio-Rad Laboratories, Hemel Hempstead, UK). One randomly selected microscopic field (2600 µm² each) from the external zone of ME of each animal was analysed, to quantify co-localization of D3 with the different peptides in the axon varicosities.

Coronal 10 µm-thick sections through the anteroposterior extent of the ME of rats perfused with 4% PFA in PBS were subjected to immunofluorescent-labelling either for GnRH, D3 or RAB3 marker. Axon varicosities located in the external zone of the ME were imaged using a Nikon N-STORM super-resolution microscope system (Nikon Instruments Ltd.), and diameter of at least 500 immunoreactive clusters from each staining was measured with the NIKON NIS software.

Developmental expression of D2, Nkx2.1, D3 and proTRH mRNA was studied with isotopic *in situ* hybridization. 12µm native chicken brain coronal sections were cut on cryostat and mounted on glass slides. After pre-hybridization treatments one of the previously mentioned targets was hybridized overnight at 65°C with 500-1000bp, S³⁵ labelled, antisense cRNA probe. Radioactive signal was detected after exposure for different time intervals with Kodak Autoradiographic Emulsion. Densitometric analysis of proTRH *in situ* hybridization signal was performed with ImageJ software on E19 and P2 sections, measuring mean silver grain density over chicken PVN.

1.7 *Deiodination assay*

Enzyme activity measurement is based on the determination of the amount of free I¹²⁵ removed by D2 from the outer ring of I¹²⁵ labelled T4, *in vitro*, in tissue lysates. The technique was used to determine D2 activity in developing chicken HT and MBH, and to detect changes in D2 activity in cold stressed iBAT after sympathetic denervation. Snap frozen tissue samples were homogenized in PE buffer (0.1M potassium phosphate, 1 mM EDTA, pH 6.9) containing 0.25M sucrose and 10 mM DTT). Equal amounts of total protein was mixed with assay buffer containing the I¹²⁵ labelled T4, and incubated on 37⁰C for the practical time. Amount of free I¹²⁵ produced by a defined protein amount and known time was determined with gamma-counter.

1.8 *Luciferase enzyme activity measurements in tissue samples and live animals*

Firefly luciferase enzyme activity can be determined *in vitro* from cell extracts, and from lysates of luciferase expressing tissues in microplate, by adding Luciferase Assay Reagent containing ATP and luciferin substrate, and measuring the light produced by the luciferase with Luminoskan Ascent luminometer. This technique was used to measure promoter activity of chicken *Dio2* promoter in response to Nkx2.1 transcription factor in U87 glioma cell line, and measure luciferase activity in THAI-Mouse tissues in response to modulation of systemic TH levels.

Luciferase activity was also detected and quantified in T3 treated, euthyroid, hypothyroid and cold stressed (24h at 4°C) live THAI-Mouse using IVIS Lumina II In vivo Imaging System. Live imaging was obtained in ketamine-xylazine anaesthetized mice whose fur over the iBAT and abdominal organs had been removed. D-luciferin was *i.p.* injected (150 and 750 µg/g bw, in PBS for the T3-treated and cold-stressed animals, respectively) 15 min before imaging.

Emitted light from the examined organ was quantitated in all animals using a region of interest (ROI) of identical size and shape.

1.9 Taqman real-time quantitative PCR

Gene expression changes were analysed with Taqman real-time PCR reactions on snap frozen tissues. TSH β mRNA was detected in T3, T4 and vehicle treated E19 and P2 chicken pituitaries. In THAI-Mice, intact and denervated iBAT was analysed for D2, luciferase mRNA in response to cold stress and D2, luciferase, and TRH was quantified in punched brain areas of LPS treated mice. Total RNA was isolated with phenol-chloroform based column purification, with RNeasy Lipid Tissue Mini kit according to manufacturer's instructions. 1 μ g total RNA was reverse transcribed with High-Capacity cDNA Reverse Transcription Kit. 10ng cDNA was applied in each Taqman reaction, using Taqman Gene expression probe sets designed by Thermo Fisher Scientific, and Taqman Fast Universal PCR Mastermix. Gene expression of target genes was compared to GAPDH housekeeping gene.

1.10 Statistics

All data are shown as mean \pm SEM. Groups were compared with two-tailed t-test. Multiple comparisons were made by one way ANOVA followed by Newman-Keuls or (above group number higher than 3) the Tukey post-hoc tests. Results of denervated iBAT experiments were analysed by Repeated Measurements ANOVA followed by Tukey post-hoc test.

IV. RESULTS

1. Regulation of the onset of negative feedback in the developing chicken hypothalamus

1.1 *T4 induced negative feedback of the chicken HPT axis forms between E19 and P2*

First we aimed to determine the period of onset of hypothalamic negative feedback, and we studied the responsiveness of proTRH expression in the PVN to T4 and T3 challenges in different developmental stages. *In situ* hybridization revealed that whereas exogenous T4 did not induce a statistically significant inhibition of proTRH expression in the PVN at embryonic day (E)19, T4 treatment was effective at two days after hatching (P2) and decreased proTRH expression by 25%. In contrast, proTRH expression responded to T3 treatment in both age groups and decreased proTRH expression by 30% in E19 chicken PVN and by 25% in P2. TSH β mRNA expression in the pituitary responded to T4 and T3 in a similar age dependent manner and reduced TSH β mRNA by 60% and 20%, respectively in P2 animals, while none of the treatments affected TSH β expression in E19 pituitary.

1.2 *The role of hypothalamic TH metabolism in the onset of negative feedback on TRH neurons*

The presented difference between the responsiveness of TRH expression in the PVN to T4 and T3 at E19 suggested that developmental changes in hypothalamic TH activation and inactivation could be an important factor in set point generation. First we focused on the local TH activation and assessed the expression of D2 mRNA in the chicken hypothalamus with isotopic *in situ* hybridization during development before and after the onset of negative TH feedback. Faint D2 hybridization signal was observed well before set point formation, in E13 β -tanycytes in the “posterior” hypothalamic sections, and in perivascular elements throughout the hypothalamus. In P2 animals, the D2 mRNA expression appeared in β -tanycytes in “anterior” regions and expanded to α -tanycytes generating an expression pattern along the ependymal layer of the third ventricle. D2 activity was also assessed both in the MBH and in the MBH-lacking hypothalamic region at stage E15, E18, and P2 with *in vitro* deiodination assay. D2 activity showed an 11.6-fold increase in the MBH and a markedly lower but significant 3.9-fold increase in the MBH-lacking hypothalamic sample when P2 samples were compared to those of E15.

We also assessed the expression and protein level of inactivating D3 but could not observe marked changes before and after the period of negative feedback formation neither in neurons nor in tanycytes which are expressing D3 abundantly in all investigated ages.

1.3 Nkx2.1 mRNA was expressed in the chicken tanycytes but not in perivascular elements

We also tried to identify factors that could be involved in the expression of D2 in the developing hypothalamus. Since the Nkx2.1 developmental transcription factor can transactivate thyroid-specific genes and human DIO2 gene, it is a potential regulator of chicken D2 expression. *In situ* hybridization revealed, that distribution of Nkx2.1 expression overlapped with that of D2 in E13 and P2 tanycytes both in the floor and the wall of the third ventricle, but Nkx2.1 was absent in D2-expressing cells of the perivascular space. To assess whether the coexpression of Nkx2.1 and D2 in chicken tanycytes could lead to Nkx2.1-mediated transcriptional activation of the chicken *Dio2* gene, we performed promoter assay in U87 glioma cells. Nkx2.1 coexpression increased transcription of the *cDio2* 3.6kb and 588 bp long 5' flanking regions by ~4-fold and 1.8-fold, respectively. The empty pGL3-basic vector remained unresponsive. Sequence analysis of the used *cDio2* 5' FR fragment indicated five potential Nkx2.1 binding sites relative to the transcriptional start site (-18, -2872, -2587: TCAAGG; -2321, -1671; TCAAGT).

2. Thyroid hormone availability in parvocellular neurosecretory neurons of the rodent hypothalamus

2.1 Distribution and subcellular localization of D3 in the rat hypothalamus

Neurons cannot generate T3 so they need to import T3 from glial cells. Intracellular level of T3 is fine tuned in neurons by D3-mediated T3 degradation. We aimed to understand how this process works in neurosecretory neurons. Using light microscopic immunohistochemistry D3-immunoreactivity appeared as small puncta distributed unevenly in the hypothalamus. The highest density was observed in the external zone of the ME, where the axons of the hypophysiotropic neurons accumulated around the portal capillary system. D3 immunoreactivity was also observed in most hypothalamic regions including those known to project to the ME (i.e. the medial preoptic area, paraventricular and arcuate nuclei), although less intense than the ME. The punctate appearance in these regions suggested localization in

axons similar to that observed in axons in the ME as no D3 immunoreactivity was identified in neuronal perikarya.

Previous ultrastructural studies of our group localized D3 to dense core vesicles (DCV) in axon varicosities. We continued this study by determining the topology of D3 in the DCV in the outer zone of the hypothalamic ME using N-STORM superresolution microscopy. Using immunofluorescent-labelling we found that the C-terminal portion of D3 formed immunoreactive clusters of 83.9 nm, that was significantly larger than clusters containing intravesicular GnRH clusters of 65.6 nm and slightly bigger than clusters containing RAB3 (81.4 nm), a protein covering the outer surface of the DCV. Thus N-STORM microscopy revealed that C-terminal active center of D3 is localized outside of the DCV surface and faces the cytoplasm, representing the main TH inactivation locus in the axon terminals. Importantly, DCV associated D3 is catalytically active in the axon terminals, as proved by the demonstration of authentic D3 activity using deiodinase assay on microdissected rat ME samples containing the axonal compartment of hypophysiotropic neurons. Furthermore, D3 activity was upregulated by ~4-fold in hyperthyroid rats.

2.2 *Phenotype of D3-immunoreactive hypophysiotropic terminals and distribution of D3 in neurosecretory neurons under pathophysiological conditions*

To determine the phenotype of the D3-containing axon terminals in the ME, co-localization of D3-immunoreactivity with hypophysiotropic releasing or inhibiting hormones was performed with double-labelling immunofluorescence and confocal microscopy. The D3-immunoreactive loci appeared as small islands within axon varicosities. D3-immunoreactivity was observed in GnRH (71.8±3.8%), CRH (63.2±7.5%), GHRH (64.2±2.7%) and TRH (26.6±5.0%) axon terminals, mostly in distal varicosities and terminal portions. The lower D3 occurrence in TRH axons was significantly different from that observed in GnRH, CRH and GHRH axons, and D3 was absent from somatostatin (SST)-immunoreactive axon varicosities and magnocellular neurons. We demonstrated that uptake of T3 is possible to hypophysiotropic axon varicosities as monocarboxylate transporter 8 (MCT8) TH transporter was presented on all types of axon terminals.

D2-mediated TH activation capacity in MBH is known to be increased in LPS-induced NTIS model, and we aimed to assess how the T3 degradation capacity of parvocellular neurons is affected by this challenge. We studied the distribution of D3 in axon terminals of parvocellular neurons 12h after *i.p.* LPS injection. LPS significantly decreased the number of D3 positive

varicosities both in GHRH (10%) and CRH (25%) containing axons suggesting decreased T3 degradation and elevated T3 level in these compartments. Importantly, neither TRH, nor GnRH-containing axons were affected. The unchanged axonal D3 content of TRH neurons after LPS challenge along with the similarly unchanged number of MCT8 positive terminals of these neurons are indicating that TRH neurons are programmed to rely on hypothalamic T3 without significant further intracellular modulation of their T3 content.

3. Generation and characterization of Thyroid hormone action indicator mouse model

3.1 Generation

TH action is a net result of the activity of a complex molecular machinery that includes TH transport, TH metabolism and TR-mediated nuclear events. To assess tissue-specific mammalian TH action in an *in vivo* context we generated a TH action indicator (THAI) mouse model and started to use in the investigation of TH signalling in the hypothalamus and iBAT. Mice were generated to assess tissue-specific TH action by expression of firefly luciferase reporter gene, which was made TH sensitive by triplets of TRE elements of hDIO1 gene. (For detailed description of targeting DNA construct see section III/1.2) Genomic insertion of the transgenic cassette was performed with pronuclear injection in the presence of *in vitro* transcribed mRNA encoding the Sleeping Beauty transposase.

Three transgenic mouse lines were generated, i.e. #4, #18 and #23. Fluorescence *in situ* hybridization revealed that homozygotes of all lines harbour two copies of the THAI transgenic construct indicating that a single copy was inserted into founders. Adult animals of the three founders are biochemically euthyroid with normal fT4 and fT3 serum concentrations, and have normal bodyweight. Splinkerette PCR revealed, that the reporter cassette was inserted into a region of repeat family L1 into the genome of THAI-Mouse line #4 indicating that the cassette did not alter the structure of any endogenous gene. In accordance, the animals did not exhibit any identifiable phenotype. In THAI-Mouse #4, neither body weight nor systemic parameters highly dependent on thyroid status (lean body mass, fat mass, respiratory exchange ratio /RER/ and volume of oxygen consumption /VO₂/) were significantly different from wild-type controls.

3.2 Characterization of TH responsiveness in THAI-Mouse lines

Various tissues of homozygote male mice with modulated TH status were harvested and processed for measurement of luciferase activity. In all lines, basal luciferase activity varied

extensively among different tissues. Differences of ~6-orders of magnitude were observed between liver and testicle, while values of most tissues fall into a range within 2-orders of magnitude. These differences are likely to reflect the overall transcriptional activity of the DNA insertion site, which is cell-specific. Line #4 exhibited a great deal of variability in tissue responsiveness to TH when treated with L-T4, from 0.8-fold in the testicle, 1.5-2 fold in brain (hypothalamus, hippocampus, cerebellum, cortex), to 64-fold in iBAT, while other highly responsive tissues were skeletal muscle, heart, mandibular salivary gland (MSG) and skin (4-11-fold). The pattern of TH responsiveness was distinct in the other THAI-Mice, with line #23 only exhibiting a ~7-fold L-T4 responsiveness in the iBAT and no detectable activity at all in this tissue of line #18. However, line #23 and #18 exhibited marked response to TH in the pituitary, and line #18 showed the highest brain baseline activity.

Thus, line #4 permits the study of TH action in a wide variety of tissues, whereas the two other lines hold additional value for specific applications represented by high reporter response in the pituitary (lines #18 and #23) and higher basal activity in the brain (#18) due to their different insertion sites.

We also tested the responsiveness of the THAI-Mouse #4 to a decrease in tissue TH action. Animals were chemically rendered hypothyroid and luciferase activity was measured in various tissues and brain regions. Approximately 2-3 fold decrease in TH signalling could be detected in different brain regions (e.g. the hypothalamus and cerebral cortex), the liver and in white blood cells, 4-6 fold in iBAT, pituitary, heart, bone and 10-fold in small intestine. Thus THAI-Mouse allows detection of tissue hypothyroidism in various tissues.

3.3 *TH signalling can be assessed in the live THAI-Mouse*

Tissues like iBAT, small intestine, MSG, skin, *saccus caecum* can be examined also in live animal, using *in vivo* bioluminescence imaging. Hypo-, eu-, and hyperthyroid #4 mice were analysed in anesthesia 15 min after *i.p.* D-luciferin injection. In the duodenum and jejunum, hypothyroidism decreased luciferase activity by ~80%. A single L-T3 injection 24h before imaging induced luciferase activity in iBAT by ~9-fold, in the small intestine by ~3-fold, and to a lesser extent in foot pads and tail.

3.4 *Application of THAI-Mouse to study tissue-specific TH signalling*

The THAI-Mouse allowed us to address the pathogenesis of NTIS by direct assessment of tissue-specific TH action in discrete brain regions. LPS induced NTIS evoked ~2 fold increase in D2 mRNA level in microdissected MBH of #23 THAI-Mouse in all investigated time points

(6, 8, 10h after *i.p.* LPS injection), that was followed by the increase of luciferase reporter expression reaching significance after 8h, at the time point when TRH expression decreased significantly by ~50% in PVN. These findings revealed that during the pathogenesis of NTIS D2-mediated increase of local TH activation affects TH signalling in the MBH that contributes to the down-regulation of the HPT axis by decreasing TRH expression in PVN.

The iBAT is under synergistic control of NE and TH signalling and is under the regulation of the central nervous system. In live #4 THAI-Mouse we could gauge physiological changes in TH availability, and detected increased TH action after 9 and 24h cold stress in iBAT. A 3.2-fold increase in bioluminescence signal was observed in iBAT after 24h of cold exposure, while foot pad skin remained unchanged. Similar induction of TH action was measured in dissected, cold stressed iBAT samples. We used this model to study the role of NE signalling in the regulation of TH action of the iBAT. Unilateral sympathetic denervation did not influence basal D2 activity and luciferase mRNA, indicating that baseline TH action is less dependent on the sympathetic input. Denervation resulted in diminished response of iBAT to cold stress, and prevented the 9-hour cold exposure induced ~2-fold increase of NE content, 9-fold increase in D2 expression and 18-fold acceleration in D2 activity that induced only ~2.7-fold increase in luciferase mRNA level in the intact iBAT lobe. Therefore we concluded that basal and cold-induced TH actions are differently regulated by the sympathetic nervous system.

The THAI-Mouse is also useful to test the performance of TR isoform-specific TH analogues, called thymimetics, which are developed to evoke the beneficial effects of TH (e.g. lowering of cholesterol and induce weight loss) without unwanted cardiac effects. Treatment of #4 THAI-Mouse with TR β isoform-specific GC24 compound increased luciferase activity by ~2.5-fold in TR β dominant liver however it did not increase TH signalling in the TR α dominant heart.

V. CONCLUSIONS

The presented results aimed to contribute to the better understanding of mechanisms underlying TH action in the developing and adult brain and in related peripheries along with the generation of a novel transgenic mouse model for these studies.

TH-mediated hypothalamic set point formation is poorly understood despite its fundamental impact on TH economy and consequently on tissue function persisting throughout the entire lifespan. Our studies in chicken model determined the period of set point formation and demonstrated that tight regulation of local hypothalamic TH availability via a dramatic developmental increase in hypothalamic D2-mediated T3 generation plays a crucial role in the formation of negative feedback on TRH neurons. Since maternal TH status impacts fetal TH availability and altered TH levels during development could result in shifted HPT set point with persisting effects, our data could provide novel arguments to the ongoing debate whether maternal TH levels should be routinely monitored during human pregnancy, especially in the sensitive period when set point of the HPT axis is formed. Studies on primates would be useful to confirm the importance of the presented mechanism in higher vertebrates.

Neurosecretory neurons represent a major hypothalamic target of TH. The revealed abundant presence of functional D3 in axon terminals of hypophysiotropic parvocellular neurons on the outer surface of dense core vesicles represents a novel regulation of neuroendocrine axes by TH. We could classify two types of axon terminals based on their D3 content. Number of D3-positive axon varicosities was found highly variable in different neurosecretory systems and was subjected to intense and quick changes in response to challenges like bacterial LPS-induced inflammation. This indicated the existence of axon-type specific regulation of intracellular T3 availability in axon terminals of neurosecretory neurons. Tanycyte processes in the median eminence represent the main source of hypothalamic T3 while the cell bodies of hypophysiotropic neurons are located in distinct brain nuclei. Thus it can be hypothesized that the pathway along TH can gain access to the nuclear compartment of these neurons involves uptake by axon terminals in the median eminence and retrograde transport along neurosecretory axons to the soma. We suggest that D3-mediated T3 inactivation in the varicosities can serve as a gate keeper that dynamically regulates the amount of T3 reaching the nucleus by retrograde transport. Furthermore D3 may have also local effect on axonal neurosecretion by affecting mitochondrial biogenesis, and function, however more studies are still needed to support this hypothesis. Monocarboxylate transporter 8-mediated axonal T3 uptake and neuron-type specific regulation of intracellular T3 concentration via D3 in the

rodent median eminence could represent a novel pathway for the modulation of hypothalamic control of reproduction, growth, stress and metabolism.

The generated Thyroid Hormone Action Indicator (THAI) Mouse model has the potential greatly facilitate the investigation of tissue-specific TH action by providing an unbiased *in vivo* model for these studies. The THAI-Mouse model is based on a firefly luciferase reporter and uses a fully endogenous set of regulators of TH action. The model allows quantification of TH action in a live mammal for the first time along with the assessment of TH action in samples originating from various brain regions and peripheral tissues. While endogenous TH responsive genes are also controlled by various non-TH related factors, THAI-Mouse authentically reports TH action. The model can detect endogenous changes in TH availability and reports both tissue hyper- and hypothyroidism in the brain and in peripheral tissues. Using this model we could demonstrate that TH action is tissue-specifically regulated in hypothalamic subdivisions during the development of infection-induced non-thyroidal illness syndrome. The model was also used to better understand TH regulated mechanism in the cold-induced iBAT. Moreover our studies demonstrated, that THAI-Mouse could be used in testing TR isoform-selective compounds in the presence of endogenously expressed receptors, and could support the efforts to develop thyromimetics to treat obesity, and high cholesterol levels. THAI-Mouse could be also highly useful to study tissue hypothyroidism during TH replacement therapy. These studies can provide novel data to advance the ongoing debate on TH replacement that could potentially affect future treatment of tens of millions of patients worldwide.

VI. LIST OF PUBLICATIONS

List of publications the thesis is based on

1. Mohácsik, P., Füzesi, T., Doleschall, M., Szabó, AS., Vancamp, P., Hadadi, É., Darras, VM., Fekete, C., Gereben, B. 2016. Increased thyroid hormone activation accompanies the formation of thyroid hormone dependent negative feedback in developing chicken hypothalamus. *Endocrinology* 157(3):1211-211.
2. Kalló, I*, Mohácsik, P*,Vida, B., Zeöld, A., Bardóczy, Z., Zavacki, AM., Farkas, E., Kádár, A., Hrabovszky, E., Arrojo e Drigo, R., Dong, L., Barna, L., Palkovits, M., Borsay, B.A., Herczeg, L., Bianco, A.C., Liposits, Z., Fekete, C., Gereben, B. 2012. A novel pathway regulates thyroid hormone availability in rat and human hypothalamic neurosecretory neurons. *PLoS One* 7: (6) Paper e37860. 16 p. *equally contributed
3. Mohácsik, P., Zeöld, A., Bianco, AC., Gereben, B. 2011. Thyroid hormone and the neuroglia: both source and target. *Journal of Thyroid Research, Special issue: Thyroid Hormones and Their Receptors: From Development to Disease* Article ID 215718, 16 pages doi:10.4061/2011/215718
4. Mohácsik, P, Erdélyi, F., Szabó, G., Fekete, Cs. and Gereben, B. (Inst. of. Exp Med., Hung. Academy of Sciences) 2016. Thyroid hormone action indicator transgenic mouse and recombinant DNA construct Hungarian Patent Claim #P1400563, International Patent Application No. PCT/HU2015/050020

Other publications

1. Wittmann, G., Szabon, J., Mohácsik, P., Nouriel, S., Gereben, B., Fekete, C., and Lechan, R. 2015. Parallel regulation of thyroid hormone transporters OATP1c1 and MCT8 during and after endotoxemia at the blood-brain barrier of male rodents. *Endocrinology* 156(4):1552–1564
2. McAninch, E., Jo, S., Preite, N., Farkas, E., Mohácsik, P., Fekete, C., Egri, P., Gereben, B., Li, Y., Deng, Y., Patti, M., Zevenbergen, C., Peeters, R., Mash, D., and Bianco, A. 2015. Prevalent polymorphism in thyroid hormone-activating enzyme leaves a genetic

fingerprint that underlies associated clinical syndromes. *The Journal of Clinical Endocrinology and Metabolism* 100(3): 920-33

3. Wittmann, G., Mohácsik, P., Balkhi, MY., Gereben, B., Lechan, RM. 2015. Endotoxin-induced inflammation down-regulates L-type amino acid transporter 1 (LAT1) expression at the blood-brain barrier of male rats and mice. *Fluids and Barriers of the CNS* 12: p. 21.

4. Fonseca, TL., Fernandes, GW., McAninch, EA., Bocco, BM., Abdalla, SM., Ribeiro, MO., Mohácsik, P., Fekete, C., Li, D., Xing, X., Wang, T., Gereben, B., Bianco, AC. 2015. Perinatal deiodinase 2 expression in hepatocytes defines epigenetic susceptibility to liver steatosis and obesity. *PROC NATL ACAD SCI USA* 112(45):14018-23

5. Rafael Arrojo e Drigo, Fonseca, TL., Castillo, M., Salathe, M., Simovic, G., Mohácsik, P., Gereben, B., and Bianco, AC. 2011. Endoplasmic reticulum stress decreases intracellular thyroid hormone activation via an eIF2a-mediated decrease in type 2 deiodinase synthesis. *Molecular Endocrinology* 25(12): 2065-2075

Σ IF: 33,426

VII. ACKNOWLEDGEMENTS

First of all I would like to express my gratitude to my tutor, Dr. Balázs Gereben, who supported tirelessly my professional improvement in his laboratory, supervised my activity with his comprehensive knowledge and serene and calm attitude to life and science while at the same time providing me freedom in work.

I am also very grateful to Dr. Csaba Fekete for his help to extend my technical background and carry out experiments.

I wish to express my thanks to Professor Zsolt Liposits, Head of the Department of Endocrine Neurobiology for his support of my progress in scientific research.

I would like to express my deepest thank to Antonio C. Bianco (Chicago, USA), Veerle M. Darras (KU Leuven, Belgium) and their research groups for the successful collaboration.

I am very thankful to Andrea Juhász, Erzsébet Farkas, Anett Szilvássy-Szabó, Dr. Csilla Molnár, for friendly atmosphere and cooperation in work.

I also thank my colleagues in the Laboratory of Molecular Cell Metabolism for the scientific discussions: Péter Egri, Dr. Anikó Zeöld, Richárd Sinkó, Dr. Anna Kollár

I would like to thank to the members of the Lendület Laboratory of Integrative Neurobiology, and the Laboratory of Endocrine Neurobiology for supporting my research with productive cooperation: Dr. Andrea Kádár, Györgyi Zséli, Dr. Mónika Tóth, Dr. Edina Varga, Dr. Barbara Vida, Dr. Tamás Füzesi, Ágnes Simon Veronika Maruzs Dr. Erik Hrabovszky, Dr. Imre Farkas, Dr. Imre Kalló, Dr. Miklós Sárvári, Dr. Csaba Vastagh, Zsuzsanna Bardóczy, Flóra Bálint, Dr. Katalin Skrapits, Barna László, Márta Turek

Special thanks to László Barna from the Nikon Microscopy Center for his supporting and technical advices in different microscopic technics.

I would like to thank for the workers of the Medical Gene Technological Unit, especially Ferenc Erdélyi, Zsuzsanna Erdélyi, Mária Kaziné Szűcs, Rozália Szafner, who helped me to learn, how to work carefully and effectively with small animals.